Supporting Information

Mechanistic Insights into UV/H_2O_2-Aged Polystyrene Enable an Optimized Protocol for Fungal Biodegradation

Zhi Guo[1,3,*], Yuanyuan Zha[1,3], Xingpan Guo[2,*], Xinlei Ling[1,3], Lin Yao[1,3], Lishou Han[1,3], Fan Yang[1,3]

[1] School of Resources and Environmental Engineering, Hefei University of Technology, Hefei 230009, China

[2] State Key Laboratory of Estuarine and Coastal Research, East China Normal University, 500 Dongchuan Road, Shanghai 200241, China

[3] Anhui Ecological Civilization Research Institute, Hefei University of Technology, Hefei 230009, China

* Corresponding author

E-mail address: guozhi@hfut.edu.cn (G.Z.); xpguo@sklec.ecnu.edu.cn (G.X.)

Contents

1. Supporting Methods

Text S1. Medium composition.

Text S2. Assays of the physiological and enzyme activities of *P. chrysosporium*.

Text S3 Experimental methods for transcriptome.

Text S4. Plastics metabolic process analysis.

2. Supporting Figures

Figure S1. Experimental setup diagram.

Figure S2. The entire degradation process,Visualization of the pre-treatment and biodegradation of plastic films.

Figure S3. The plastic films fragmented into irregular pieces.

Figure S4. Expression Analysis

Figure S5. Venn diagram of CK versus P-PS, CK versus UV/H_2O_2-PS, P-PS versus UV/H_2O_2-PS experimental groups.

Figure S6. Volcanic map of of CK versus P-PS, CK versus UV/H_2O_2-PS, P-PS versus UV/H_2O_2-PS experimental groups

Figure S7. CK vs P-PS bubble diagram of GO enrichment analysis.

Figure S8. CK vs UV/H_2O_2-PS bubble diagram of GO enrichment analysis.

Figure S9. P-PS vs UV/H_2O_2-PS bubble diagram of GO enrichment analysis.

3. Supporting Tables

Table S1. GC-MS results of compounds released from polymer film by UV/H_2O_2 pretreatment stage.

Table S2.GC-MS results of compounds released from polymer film by P. *chrysosporium*.

Table S3. Raw data.

Table S4. Genes relative to extracellular enzymes

Table S5. Genes relative to the enzymes involved in the degradation reactions

Table S6. Genes relative to endocytosis and vesicle transport

Table S7. Genes relative to Fatty acid degradation

Table S8. Genes relative to TCA cycle

Text S1. Medium composition.

The Potato Dextrose Agar medium was prepared for strain propagation, and the main components of the medium (20g glucose, 3g KH_2PO_4, 1.5g $MgSO_4 \cdot 7H_2O$ and 20g agar) were dissolved in 1000 ml of potato extract solution (cut potatoes into small pieces, add water to boil, and then filter with gauze to get the potato extract solution), adjust the pH of the culture solution to be weakly alkaline.

Carbon limited Potato Dextrose Agar medium was used for plastic degradation and a series of fungus experiments, (5g glucose, 3g KH_2PO_4, 1.5g $MgSO_4 \cdot 7H_2O$ and 20g agar) were dissolved in 1000 ml of potato extract solution (Cut potatoes into small pieces, add water to boil, and then filter with gauze to get the potato extract solution), adjust the pH of the culture solution to be weakly alkaline.

Text S2. Assays of the physiological and enzyme activities of *P. chrysosporium*.

The cultures and plastic films were collected during the biodegradation process. Fungal mycelia were harvested by filtration through a Buchner funnel equipped with a 0.22 μm membrane and subsequently dried in a vacuum oven at 105 °C for 24 h. The dry biomass weight was used to evaluate the colonization level of the fungus. After filtration from each Petri dish and repeated rinsing with ultrapure water (2–3 times), white-rot fungal mycelia with a fresh weight of 0.2 g were transferred into a 10 mL centrifuge tube. One milliliter of thiazole blue (MTT) solution (80 mg/L) was added to each tube, and the tubes were incubated in a water bath at 50 °C for 2 h. Then, 0.5 mL of hydrochloric acid solution (1 mol/L) was immediately added to terminate the reaction. The samples were centrifuged at 10,000 rpm for 5 min using a high-speed refrigerated centrifuge. After centrifugation, the supernatant was collected, mixed with 8 mL of isopropyl alcohol, and the absorbance at 534 nm was measured using a UV spectrophotometer after 2 h of shaking in the dark. The cellular activity of each sample was calculated as the ratio relative to the control group (without plastics).Weigh 0.3 g of bacterial cells (wet weight) into a 2-mL centrifuge tube. Add 1.5–1.7 mL of PBS buffer. Centrifuge at 12,000 rpm at 4°C for 10 minutes. Collect the supernatant and filter through a water-permeable membrane to obtain the crude enzyme solution.

MnP activity was determined as follows. First, 2.4 mL of succinic acid buffer (0.05 M, pH 4.5) and 0.1 mL of $MnSO_4$ (15 mM) were mixed thoroughly, and 0.4 mL of crude enzyme extract was then added. The reaction was initiated by adding 0.1 mL of H_2O_2 (10 mM). The change in absorbance at 290 nm over 3 min was monitored. One unit (U) of MnP activity was defined as the amount of enzyme required to produce 1 μmol of Mn^{3+} per minute at 37 °C and pH 4.5.

LiP activity was determined as follows. A total of 1.5 mL of tartaric acid buffer (0.1 M, pH 3.0) and 1.0 mL of veratryl alcohol solution (100 mM) were thoroughly mixed, followed by the addition of 0.4 mL of crude enzyme extract. The reaction was initiated by adding 0.1 mL of H_2O_2 (10 mM). The change in absorbance at 310 nm over 3 min was recorded. One unit (U) of LiP activity was defined as the amount of enzyme required to produce 1 μmol of veratryl alcohol oxidation product per minute.

Lac activity was determined using ABTS as the substrate. A total of 2.0 mL of sodium citrate buffer (0.1 M, pH 5.0), 0.5 mL of ABTS solution (1 mM), and 0.5 mL of crude enzyme extract were mixed at 30 °C. The change in absorbance at 420 nm was immediately measured using a UV–visible spectrophotometer. One unit (U) of Lac activity was defined as the amount of enzyme required to convert 1 μmol of ABTS per minute.

Text S3 Experimental methods for transcriptome.

1. RNA detection

Total RNA was extracted, and residual DNA was removed using the RNA Kit (15NT) (Agilent, DNF-471-1000). RNA integrity was assessed using RNA-specific agarose gel electrophoresis or an Agilent 2100 Bioanalyzer with the RNA 6000 Nano Kit (Agilent, 5067-1511).

2. Library construction process

Sequencing libraries were generated using the TruSeq RNA Sample Preparation Kit (Illumina, San Diego, CA, USA). Firstly, mRNA was purified from total RNA using poly-T oligo-attached magnetic beads. Fragmentation was carried out using divalent cations under elevated temperature in an Illumina proprietary fragmentation buffer. First strand cDNA was synthesized using random oligonucleotides and Super Script II. Second strand cDNA synthesis was subsequently performed using DNA Polymerase I and RNase H. Remaining overhangs were converted into blunt ends via exonuclease/polymerase activities and the enzymes were removed. After adenylation of the 3′ ends of the DNA fragments, Illumina PE adapter oligonucleotides were ligated to prepare for hybridization. To select cDNA fragments of the preferred 400-500 bp in length, the library fragments were purified using the AMPure XP system (Beckman Coulter,Beverly, CA, USA). DNA fragments with ligated adaptor molecules on both ends were selectively enriched using Illumina PCR Primer Cocktail in a 15 cycle PCR reaction. Products were purified (AMPure XP system) and quantified using the Agilent high sensitivity DNA assay on a Bioanalyzer 2100 system (Agilent). The sequencing library was then sequenced on NovaSeq 6000 platform (Illumina) by Shanghai Personal Biotechnology Cp. Ltd.

Databases used for gene function annotation include NR, GO, KEGG, eggNOG, Swiss-Prot, Pfam.

3. Expression analysis

Using transcriptome expression quantification software RSEM (v2.15), Clean Reads of each sample were compared to the reference sequence using the spliced unigene sequence as reference. Then the number of Reads from each sample to each gene was counted, and the FPKM value of each gene was calculated.

4. Differential gene analysis

DESeq (v1.38.3) software was used to analyze the differential expression between the two comparison combinations. DESeq was used to analyze the difference of gene expression, and the conditions for screening the differentially expressed genes were: expression difference multiple $|\log2FoldChange|>1$, the significant P-value<0.05.

5. Differential gene enrichment analysis

TopGO (v2.50.0) was used for GO enrichment analysis, P-value was calculated by hypergeometric distribution method (the standard of significant enrichment was P-value<0.05), and GO term of significant enrichment of differential genes (all/up/down) was found, so as to determine the main biological functions of differential genes. The KEGG pathway enrichment analysis was performed using clusterProfiler (v4.6.0) software, focusing on significant enrichment pathways with P-value<0.05.

Text S4. Plastics metabolic process analysis.

The biodegradation products were characterized via gas chromatography–mass spectrometry (GC–MS). First, the plastic film was removed from the Petri dish, 20 mL of deionized water was added, and the medium was stirred into a homogeneous slurry. The slurry was transferred to a 50 mL colorimetric tube, and the agitator was washed three times with 10 mL of deionized water. After the slurry was centrifuged at 3000 rpm for 10 minutes, the supernatant was transferred to 50 mL clear glass bottles. Then, 20 mL of dichloromethane (CH_2Cl_2) was added to extract the organic phase and transferred into a 20 mL glass bottle. CH_2Cl_2 was evaporated to a small volume under a nitrogen blower, and any remaining water was removed by adding 1 g of sodium sulfate (Na_2SO_4). Finally, a sample size of 1 mL was transferred into brown glass bottles in preparation for GC–MS analysis

Figure S1. Experimental setup diagram.

Figure S2. The entire degradation process,Visualization of the pre-treatment and biodegradation of plastic films.

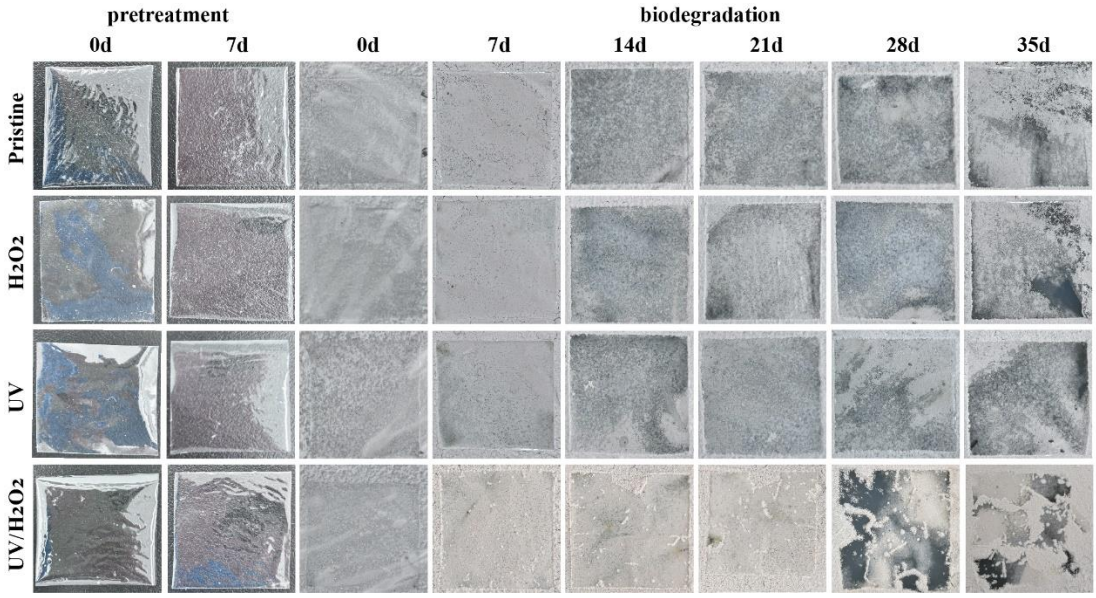

Figure S3. The plastic films fragmented into irregular pieces.

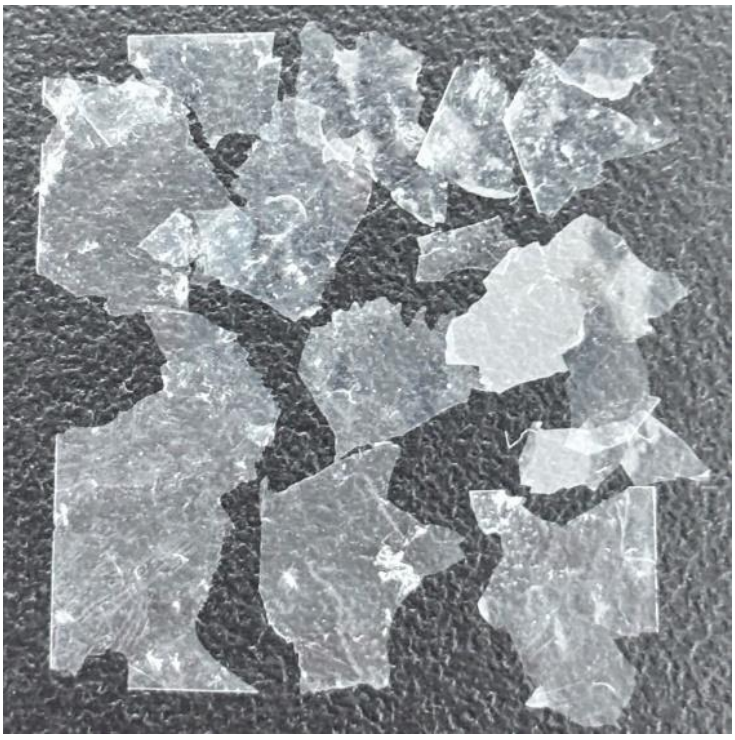

Figure S4. Expression Analysis.

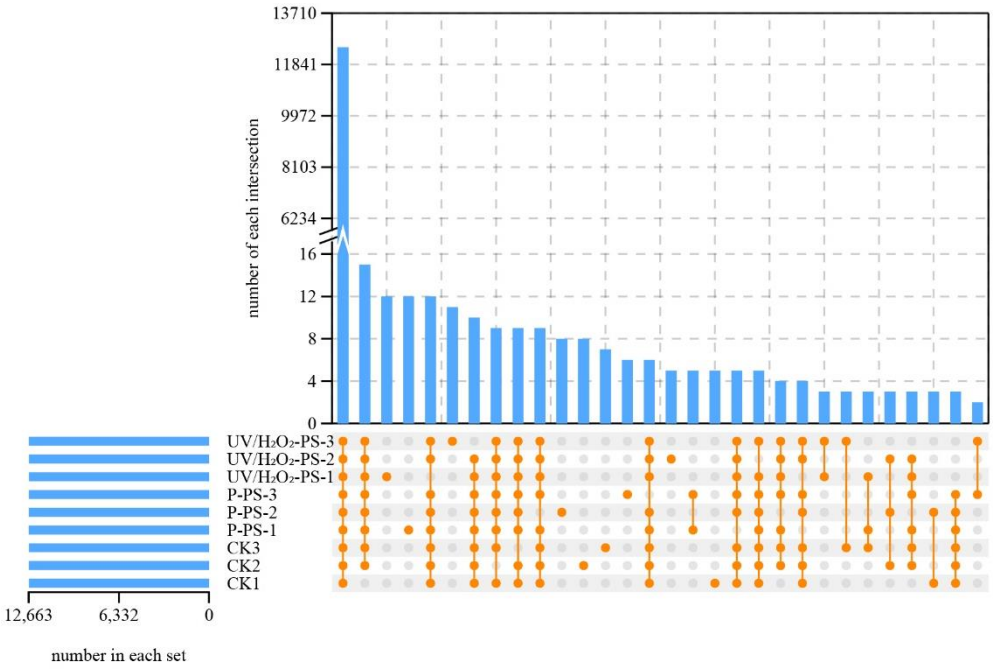

Number in each set refers to the total genes expressed in a sample.

Number of each intersection is the count of genes shared by the linked samples.

Connecting lines represent the number of overlapping genes, while individual points show the number of genes specific to that sample.

Figure S5. Venn diagram of CK versus P-PS, CK versus UV/H_2O_2-PS, P-PS versus UV/H_2O_2-PS experimental groups.

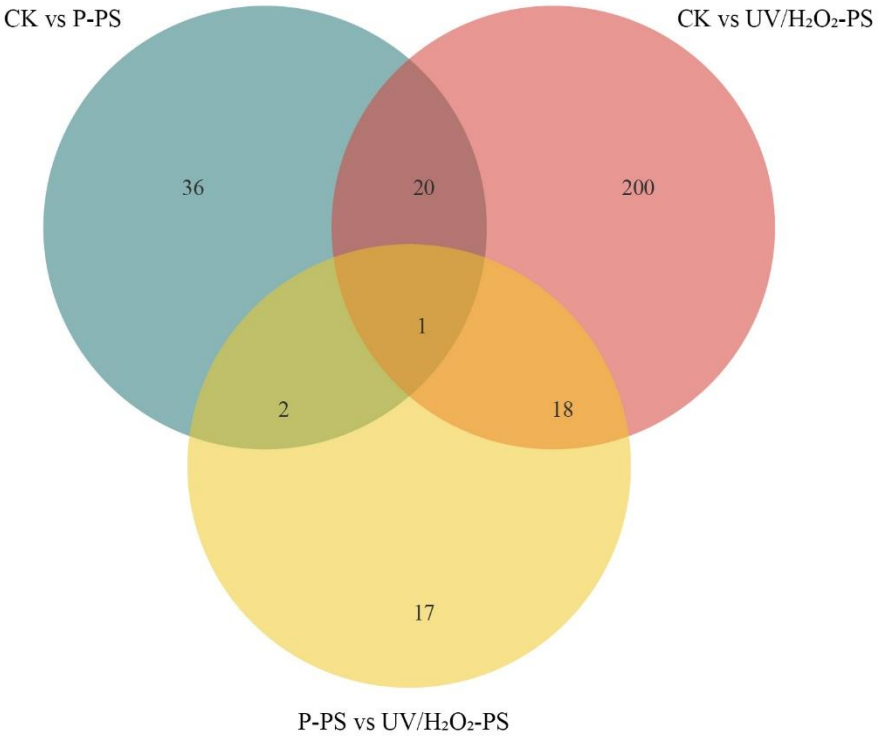

The sum of the numbers in each circle represents the total number of differential genes for that comparison set, and the overlapping part of the circle indicates the differential genes shared between the two comparison sets.

Figure S6. Volcanic map of of CK versus P-PS, CK versus UV/H_2O_2-PS, P-PS versus UV/H_2O_2-PS experimental groups ($p < 0.05$ and fold change ≥ 1.5; n = 3).

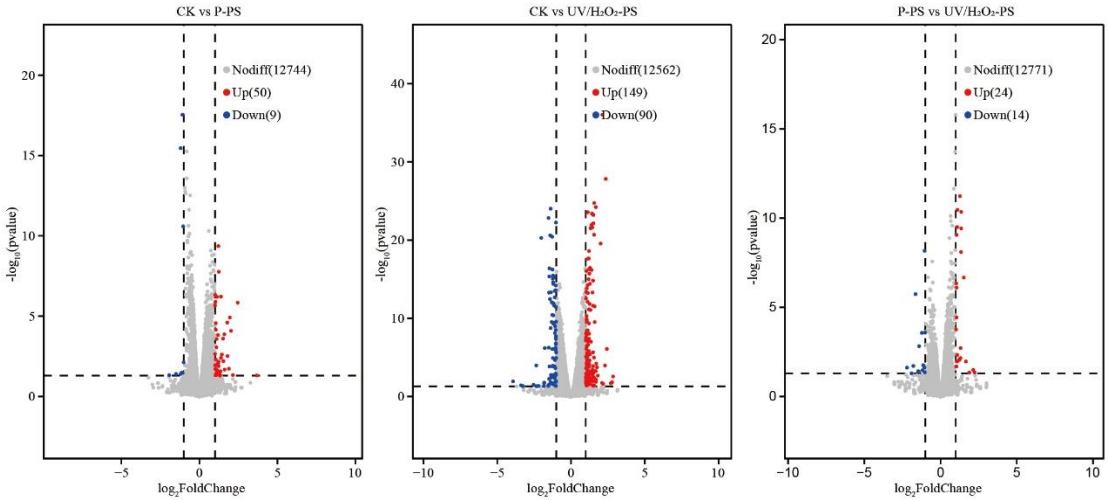

Figure S7. CK vs P-PS bubble diagram of GO enrichment analysis.

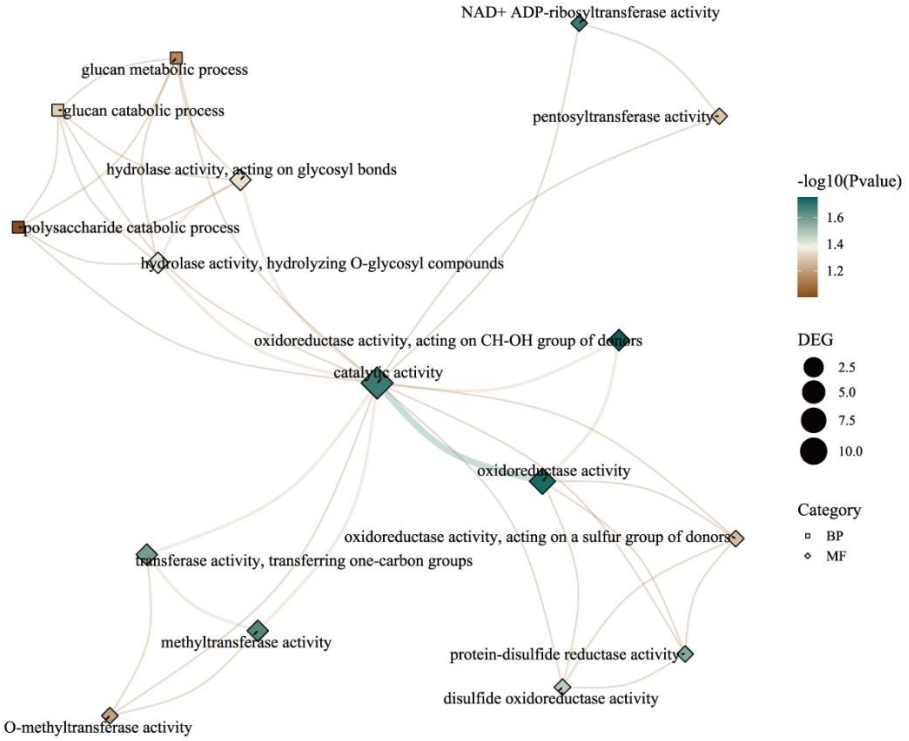

Figure S8. CK vs UV/H_2O_2-PS bubble diagram of GO enrichment analysis.

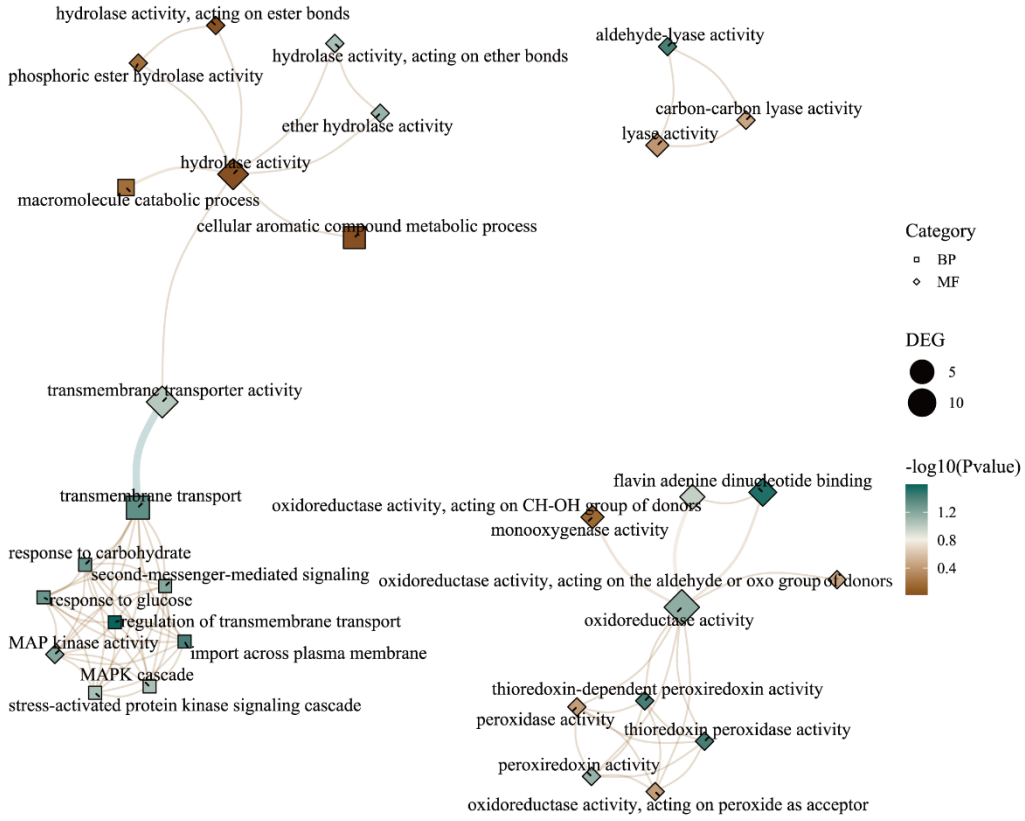

Figure S9. P-PS vs UV/H_2O_2-PS bubble diagram of GO enrichment analysis.

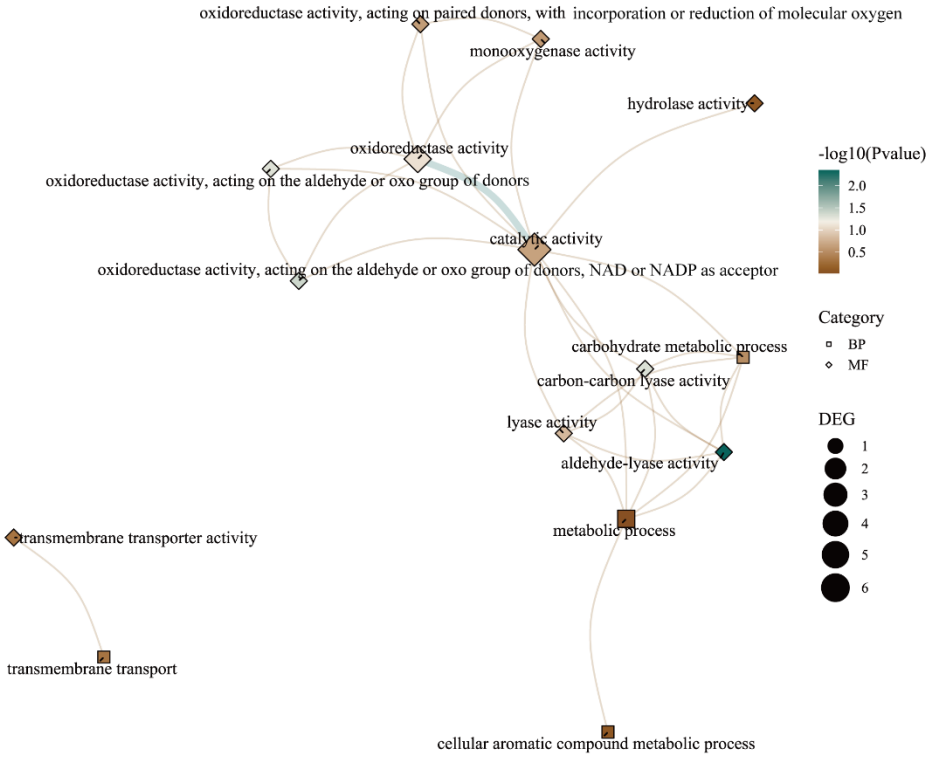

Table S1. GC-MS results of compounds released from polymer film by UV/H_2O_2 pretreatment stage.

No.	Chemical formula	Chemical formula	Structural formula	m/z (Relative intensity, %)
1	3-methyl-2-Butenal	C_5H_8O	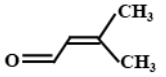	84(100),71(7),69(5),43(2),55(48)
2	Acetic acid butyl ester	$C_6H_{12}O_2$	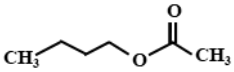	43(100),57(41),56(25),41(26),47(25)
3	4,5-Dimethoxy-2-hydroxyacetophenone	$C_{10}H_{12}O_4$	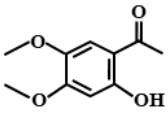	181(100),196(68),101(38),137(24),118(9)
4	4,4'-Isopropylidenediphenol	$C_{15}H_{16}O_2$	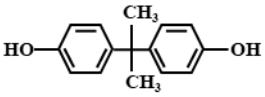	239(100),26(82),228(66),24(49),214(50)
5	2-methyl-Benzaldehyde,	C_8H_8O	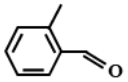	91(100),120(70),119(65),65(26), 39(17)
6	2,2,4-trimethyl-Pentane	C_8H_{18}	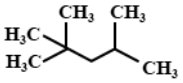	43(100),57(40),56(26),41(26),47(25)
7	1,2,4-Benzenetricarboxylic acid	$C_{11}H_{10}O_6$	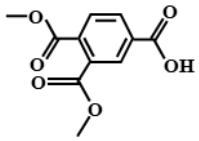	207(100),43(37),125(21),118(10),239(9)
8	2,4-Di-t-butylphenol	$C_{14}H_{22}O$	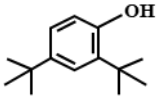	191(100),57(28),192(18),163(16),206(15)

Table S2.GC-MS results of compounds released from polymer film by *P. chrysosporium*.

No.	Chemical formula	Chemical formula	Structural formula	m/z (Relative intensity, %)
1	2-ethyl-1-butano	$C_6H_{14}O$	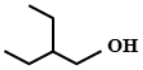	71(100),43(61),55(51),70(46),85(43)
2	(E)-3-methyl-non-3-ene	$C_{10}H_{20}$	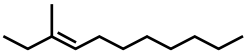	70(100),56(89),55(82),69(75),83(58)
3	3,5-dimethyloctane	$C_{10}H_{22}$	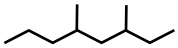	57(100), 71(91), 43(22),99(21), 84(15)
4	Decane	$C_{10}H_{22}$		57(100),43(80), 41(64), 71(44), 85(29)
5	2-isopropyl-5-methylhexan-1-ol	$C_{10}H_{22}O$	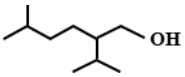	71(100),57(99),43(92),55(68),56(63)
6	3-methylundecane	$C_{12}H_{26}$	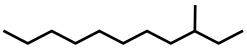	57(100),85(81),71(70), 43(48), 99(18)
7	6-ethyl-2-methyldecane	$C_{13}H_{28}$	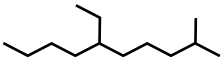	57(100), 43(76), 71(43), 85(26) 41(30)
8	dodecane,4,6-dimethyl	$C_{14}H_{30}$	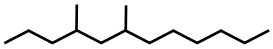	57(100), 71(90), 43(47), 85(28),70(20)
9	4-nonanone	$C_9H_{18}O$	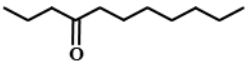	43(100),71(60),41(19),99(34),58(34)
10	cis-7-Hexadecenoic acid	$C_{16}H_{30}O_2$	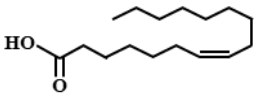	55(100), 41(62), 43(45), 69(44), 83(39)
11	2-methyl-2-phenyloxirane	C9H10O	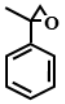	105(100),77(44),103(36), 78(33), 79(31)
12	Phenol	C_6H_6O	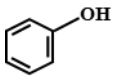	94(100),66(25),65(22),63(10),95(8)
13	m-Tolualdehyde	C_8H_8O	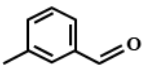	91(100),120(89),119(89),65(27),63(20)
14	3,4-Dimethylbenzaldehyde	$C_9H_{10}O$	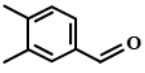	133(100),134(88),105(56),77(24),103(14)
15	4-Methoxystyrene	$C_9H_{10}O$	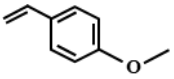	134(100),119(54),91(41),133(31),65(23)
16	4-Isopropenylphenol	$C_9H_{10}O$	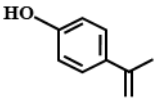	134(100),119(74),65(27),133(26),85(25)

17	4-Pentylphenol	$C_{11}H_{16}O$	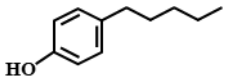	107(100),203(30),12(10),164(11),354(15)
18	hexoxybenzene	$C_{12}H_{18}O$	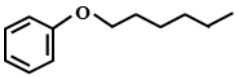	94(100),178(94),19(49),23(44)
19	Benzeneacetic acid, 2-tetradecyl ester	$C_{22}H_{36}O_2$	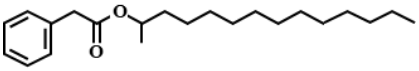	57(100), 91(86), 43(83),71(62),41(54)
20	4-Propylbiphenyl-4-Carboxylic Acid	$C_{16}H_{16}O_2$	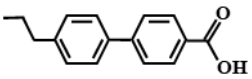	211(100),132(89),240(60),286(42)

Table S3. Raw data.

Sample	Reads No.	Raw Bases(bp)	Q30(bp)	GC(%)	N(%)	Q20(%)	Q30(%)
CK1	42653460	6440672460	6155557622	58.82	0.004292	98.93	95.57
CK2	40414154	6102537254	5830481077	58.94	0.004286	98.91	95.54
CK3	39683980	5992280980	5726999290	58.92	0.004307	98.92	95.57
PS-1	43349160	6545723160	6259428204	59.03	0.004329	98.96	95.63
PS-2	45168050	6820375550	6510263201	58.96	0.004342	98.89	95.45
PS-3	41915706	6329271606	6039601937	58.99	0.004320	98.87	95.42
UV/H_2O_2-PS-1	39393218	5948375918	5681483157	58.99	0.004283	98.93	95.51
UV/H_2O_2-PS-2	38826184	5862753784	5609165451	58.86	0.004337	98.98	95.67
UV/H_2O_2-PS-3	40224384	6073881984	5805857680	58.94	0.004307	98.94	95.59

After the sample is sequenced on the computer, the image file is obtained, which is converted by the built-in software of the sequencing platform to generate the Raw Data of FASTQ, that is, the data off the computer. The Raw Data for each sample were counted separately, including sample name, Q30, percentage of fuzzy bases, and Q20(%) and Q30(%).

CK: *P. chrysosporium* Control group;

P-PS: *P. chrysosporium* incubation with P-PS;

UV/H_2O_2-PS: *P. chrysosporium* incubation with UV/ H_2O_2-PS;

Reads No.: Reads number；

Bases(bp): Base number;

Q30 (bp): Base recognition accuracy of more than 99.9% of the total number of bases;

N (%): Percentage of fuzzy bases;

Q20(%): The percentage of bases whose base recognition accuracy is above 99%;

Q30(%): The percentage of bases whose base recognition accuracy is above 99.9%.

Table S4. Genes relative to extracellular enzymes

Gene ID	Gene name	Genes description	Fold change for P-PS	Fold change for UV/H_2O_2-PS
AGR57_14195	LPOA	AAD46494.1 lignin peroxidase	1.1426	1.2475
AGR57_7704	-	AAA33745.1 manganese peroxidase isozyme 2 precursor	1.2576	1.2815
AGR57_13022	MNP1	PEM1_PHACH Manganese peroxidase 1 OS	1.6249	1.4297
AGR57_8985	LAC1	AAS21669.1 multicopper oxidase 4A	1.0105	1.0607
AGR57_8978	fetC	AAO42609.1 extracellular multicopper oxidase	1.0295	1.2048
AGR57_14174	GLG5	LIG5_PHACH Ligninase LG5 OS	1.0316	1.2504
AGR57_14158	GLG2	LIG2_PHACH Ligninase LG2 OS	1.3959	1.2346
AGR57_1292	-	AAB39652.1 manganese peroxidase isozyme 3	1.2339	1.3276
AGR57_13026	MNP1	Q02567.1 RecName: Full=Manganese peroxidase 1	1.2604	1.1953
AGR57_8975	LAC2	AAS21662.1 multicopper oxidase 3B	0.988	1.0451

Table S5. Genes relative to the enzymes involved in the degradation reactions

Gene ID	Gene name	Genes description	Fold change for P-PS	Fold change for UV/H_2O_2-PS
AGR57_10309	YUC5	GJE89306.1 Flavin-containing monooxygenase	2.0689	1.5696
AGR57_11744	FCK2	AAX81444.1 high nitrogen upregulated cytochrome P450 monooxygenase 2	1.76	1.2678
AGR57_1127	ple1	BAL05169.1 cytochrome P450	1.6706	1.9773
AGR57_2648	CYP074	BAL05172.1 cytochrome P450	1.5811	1.7372
AGR57_2386	CYP075	AAL67905.1 cytochrome P450 monooxygenase	1.5293	1.8409
AGR57_15504	CYP091	BAL05087.1 cytochrome P450	0.8886	4.5968
AGR57_14986	CYP075	BAL05190.1 cytochrome P450	1.1877	2.3419
AGR57_6451	CYP067	BAL05193.1 cytochrome P450	1.2288	1.9929
AGR57_8204	CYP091	BAL05087.1 cytochrome P450	1.5291	1.9061
AGR57_11759	-	GJE89571.1 catechol 1,2-dioxygenase	1.4109	1.6155
AGR57_333	ipdC	GJE86950.1 2-nitropropane dioxygenase	0.9244	1.5083
AGR57_12967	oryG	GJE90676.1 TauD/TfdA family taurine catabolism dioxygenase	-	1.4664
AGR57_1091	-	GJE97923.1 aromatic compound dioxygenase	1.127	1.4282
AGR57_7451	tcpC	TCPC_CUPPJ 6-chlorohydroxyquinol 1,2-dioxygenase	1.1115	1.4189
AGR57_13921	adh	ADH2_GEOSE Alcohol dehydrogenase	2.6046	2.0721
AGR57_8919	aldA	GJE91571.1 aldehyde dehydrogenase	1.0411	1.3347
AGR57_10940	ALDH3A1	GJE86460.1 aldehyde dehydrogenase family protein	1.1726	1.1749
AGR57_7611	SPCC417.12	GJE85461.1 carboxylesterase	1.0317	1.1178
AGR57_7162	hmgA	GJE85537.1 homogentisate 1,2-dioxygenase	1.2454	1.1681

Table S6. Genes relative to endocytosis and vesicle transport

Gene ID	Gene name	Genes description	Fold change for P-PS	Fold change for UV/H_2O_2-PS
AGR57_12966	ARF	GJE96028.1 ADP-ribosylation factor-like protein	1.1754	1.6906
AGR57_3253	SPAC664.02c	GJE93211.1 actin-like ATPase domain-containing protein	1.0856	1.379
AGR57_12089	end4	SLA2_SCHPO Endocytosis protein end4	1.0113	1.0526
AGR57_4999	fcyB	GJE93171.1 NCS cytosine-purine permease	1.5475	2.7469
AGR57_359	Sft2d2	SFT2B_MOUSE Vesicle transport protein	1.2084	1.6164
AGR57_10246	vti1	GJE89440.1 vesicle transport v-snare protein vti1	0.9786	1.1473

Table S7. Genes relative to Fatty acid degradation

Gene ID	Gene name	Genes description	Fold change for P-PS	Fold change for UV/H_2O_2-PS
AGR57_9721	lcf1	GJE98644.1 long-chain acyl-CoA synthetase	0.8875	1.0055
AGR57_13921	adh	ADH2_GEOSE Alcohol dehydrogenase	2.6046	2.0721
AGR57_12373	DLD	DLD_ARATH D-lactate dehydrogenase [cytochrome]	1.562	2.1942
AGR57_552	meh	MEH_CHLAA Mesaconyl-C(4)-CoA hydratase	1.9882	2.1487
AGR57_14850	ACX1.2	GJE95425.1 acyl-CoA dehydrogenase NM domain-like protein	1.2619	1.6763
AGR57_4649	hbd	GJE94649.1 3-hydroxyacyl-CoA dehydrogenase	0.9349	0.8434

Table S8. Genes relative to TCA cycle.

Gene ID	Gene name	Genes description	Fold change for P-PS	Fold change for UV/H_2O_2-PS
AGR57_2417	PDB1	GJE84218.1 pyruvate dehydrogenase E1 component subunit beta	0.9864	1.1173
AGR57_9184	MDH1	GJE92943.1 NAD-malate dehydrogenase	1.0001	1.1153
AGR57_13252	gltA	CISYC_DICDI Citrate synthase	1.1296	1.3497
AGR57_7437	CNBA4490	GJE94825.1 succinate dehydrogenase assembly factor 2	1.1043	1.1235
AGR57_3454	pyc	GJE91041.1 pyruvate carboxylase	0.9825	1.0644
AGR57_12144	aco2	GJE85971.1 aconitate hydratase	1.0956	1.1648
AGR57_5052	icdA	IDHP_ASPNG Isocitrate dehydrogenase [NADP]	0.9792	0.9947